Doping-dependent nodal Fermi velocity in Bi-2212 revealed by high-resolution ARPES

I. M. Vishik,[1, 2] W. S. Lee,[1, 2] F. Schmitt,[1, 2] B. Moritz,[1, 2] T. Sasagawa,[3] S.
Uchida,[4] K. Fujita,[5] S. Ishida,[4] C. Zhang,[6] T. P. Devereaux,[1, 2] and Z. X. Shen[1, 2]

[1]*Stanford Institute for Materials and Energy Sciences,*
SLAC National Accelerator Laboratory, 2575 Sand Hill Road, Menlo Park, CA 94025, USA
[2]*Geballe Laboratory for Advanced Materials, Departments of Physics*
and Applied Physics, Stanford University, Stanford, CA 94305, USA
[3]*Materials and Structures Laboratory, Tokyo Institute of Technology, Meguro-ku, Tokyo 152-8550, Japan*
[4]*Department of Physics, Graduate School of Science,*
University of Tokyo, Bunkyo-ku, Tokyo 113-0033, Japan
[5]*Laboratory for Atomic and Solid State Physics,*
Department of Physics, Cornell University, Ithaca, NY 14853, USA
[6]*State Key Laboratory of Crystal Materials, Shandong University, Jinan, 250100, P.R.China*
(Dated: March 23, 2010)

The improved resolution of laser-based angle-resolved photoemission spectroscopy (ARPES) allows reliable access to fine structures in the spectrum. We present a systematic, doping-dependent study of a recently discovered low-energy kink in the nodal dispersion of $Bi_2Sr_2CaCu_2O_{8+\delta}$ (Bi-2212), which demonstrates the ubiquity and robustness of this kink in underdoped Bi-2212. The renormalization of the nodal velocity due to this kink becomes stronger with underdoping, revealing that the nodal Fermi velocity is non-universal, in contrast to assumed phenomenology. This is used together with laser-ARPES measurements of the gap velocity, v_2, to resolve discrepancies with thermal conductivity measurements.

PACS numbers:

In a d-wave superconductor like the high-T_c cuprates, the electronic component of low-temperature thermodynamics is dictated by the nodes, where arbitrarily small excitations are permitted by the gapless nature of these points. An intriguing aspect of cuprate phenomenology is the so-called universal nodal Fermi velocity (v_F).[1] Along the nodal direction $((0,0)-(\pi,\pi))$ the velocity measured by ARPES within 50 meV of E_F appears to be independent of cuprate-family or the number of CuO_2 layers in the compound, and is also nearly constant across the phase diagram – from the undoped insulator, across the superconducting dome, and in the non-superconducting metallic state at a doping $p>0.25$ – even though other electronic properties vary significantly with doping.[2–4] In addition, this universal v_F, if combined with ARPES measurement of the superconducting gap, leads to apparent contradiction with thermal conductivity observed directly in transport measurements,[5, 6] suggesting that crucial information about the nodal quasiparticles is still missing.

ARPES data can be represented as a convolution between the single-particle spectral function and the momentum and energy resolution of the experiment. Naturally, with the improved resolution of laser-based ARPES, the measured spectrum begins to approach the intrinsic spectral function, and finer structure can be revealed. Recent laser-ARPES measurements along the nodal direction of optimally-doped Bi-2212 have uncovered a low-energy (<10 meV) kink,[7] in addition to the larger kink seen at 50-80 meV in all cuprates.[8–10] Other laser-ARPES studies have shown a correspond-
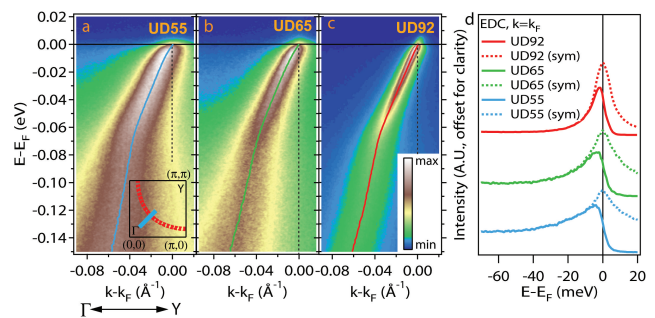

FIG. 1: (a)-(c) False-color image plots of the nodal dispersion of UD55, UD65, and UD92, measured at 10K. Solid curves indicate band dispersions derived from MDC peak positions. Inset of (a): Brillouin zone schematic with Fermi surface indicated in red. The x-axes in (a)-(c) correspond to momentum along diagonal blue line ('nodal cut') in inset. (d) EDCs (solid) and symmetrized EDCs (dashed) at k_F. A single peak at E_F in the latter confirms that spectra in (a)-(c) are ungapped. k_F determined from Fermi crossing of dispersion (vertical dashed lines in (a)-(c)).

ing decrease in nodal linewidth at low energies.[11–13] In this letter, we present the systematics of the low-energy kink by means of a doping-dependent study of underdoped Bi-2212. 20 samples with 6 dopings in the range $0.076<p<0.14$ were measured using a 7 eV laser and a Scienta SES2002 analyzer. 7 eV photons were produced by second harmonic generation from a 355 nm laser (Paladin, Coherent, Inc.) using a nonlinear crystal $KBe_2BO_3F_2$.[14] Energy and momentum resolution were 3 meV and better than 0.005 Å^{-1}, respectively. Sam-
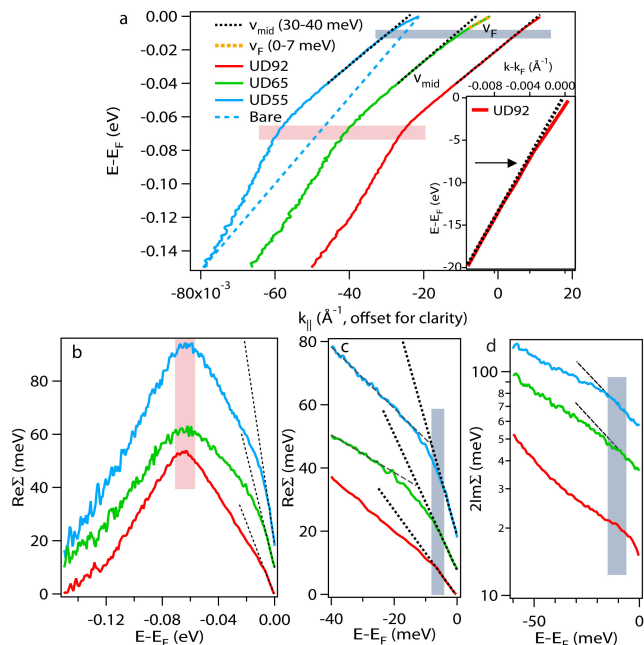
FIG. 2: (a) Band dispersions from Fig 1, offset for clarity. Dashed line accompanying UD55 denotes assumed linear bare band. Black dotted lines are linear fits 30-40 meV (v_{mid}), extrapolated to E_F. This differs from v_F (fit 0-7 meV), indicated on UD65 dispersion by orange dashed line. Pink bar marks 70 meV kink, and grey bar marks low-energy kink, where v_F deviates from v_{mid}. Inset: UD92 dispersion below 20 meV. (b) ReΣ, approximated by subtracting a linear bare band from dispersions in (a), is peaked at the position of the 70 meV kink and changes slope near the energy position of the low-energy kink. (c) Detail of the low-energy portion of ReΣ. Thick dotted lines are fits near E_F. All curves deviate from these lines between 6-10 meV, as highlighted by the shaded bar. For the two most underdoped samples, the slope of ReΣ evolves between the low-energy kink and 20-30 meV, suggesting an additional kink. (d) 2ImΣ, with dotted lines as guides-to-the-eye. All curves decrease more rapidly near E_F, but most markedly in UD92. For more underdoped samples, the effect may be obscured by a larger linewidth and possible additional kink.

ples were cleaved in-situ at a pressure $<4\times10^{-11}$ torr to obtain a clean surface, and measured at 10K.

Fig. 1(a)-(c) show ARPES image plots for nodal cuts at three dopings: UD55 (underdoped, T_c=55K), UD65, and UD92, corresponding to hole-dopings of approximately 0.088, 0.10, and 0.14. Standard momentum distribution curve (MDC) analysis–Lorentzian fits at fixed energy– is used to extract the band dispersions.[15] The energy distribution curves (EDCs)–intensity as a function of energy at fixed momentum– at k_F in Fig. 1(d) indicate that these spectra are ungapped, as the symmetrized EDCs [16] have a single peak at E_F.

The systematics of the low-energy kink are studied via the MDC-derived nodal dispersion, which are plotted for three dopings in Fig. 2(a). In addition to the large,

ubiquitous kink near 70 meV, a smaller kink is also evident: the dispersion within 10 meV of E_F deviates from the velocity fit between 30-40 meV. This deviation appears more pronounced for more underdoped samples. Consistent with the work of Plumb *et al*, the velocity (slope of the MDC dispersion) within 7 meV of E_F is *smaller* than the velocity at higher binding energy, notably opposite to the expected effects of instrument and thermal broadening.[7] We also note that the low-energy kink cannot be identified as an artifact due to a gap, because measurements are performed at the node where the superconducting gap is zero.

Another way to visualize the low-energy kink is via the real part of the electronic self-energy, ReΣ, plotted in Fig. 2(b)-(c). The low-energy kink is marked by a deviation of the slope of ReΣ at 6-10 meV from the slope established at E_F. For the sample closest to optimal doping, UD92, there is a single 'knee' in ReΣ. Meanwhile, the slope of ReΣ for UD55 and UD65 continues to evolve until 20-30 meV, possibly suggesting an additional kink, reminiscent of the 70meV kink, which may have several components.[17–19] From the Kramers-Kronig relation between ReΣ and ImΣ, a signature of the low-energy kink is expected in ImΣ, which is proportional to the MDC FWHM. In Fig. 2(d) we show that all dopings exhibit a downturn in ImΣ near E_F, though this is most pronounced for UD92. For more underdoped samples, the larger linewidth and possible additional kink make it more difficult to get quantitative information from ImΣ, but the observation that ImΣ decreases more rapidly close to E_F remains robust. The appearance of a low-energy feature in both ReΣ and ImΣ strongly argues against a spurious origin for the low-energy kink, and the phenomenology reported in Fig. 2 is reproduced in the other samples in our study. Thus, the systematics of a new energy scale can be added to the hierarchy of multiple energy scales in the cuprates.[20]

The ubiquity of the low-energy kink in UD Bi-2212 leads us to reexamine previous measurements of v_F, as there is now compelling evidence that quasiparticles very close to E_F experience a heretofore unconsidered mass renormalization. The nodal v_F is plotted in Fig. 3, and our key finding is that v_F is not universal, but rather, has a pronounced doping dependence in the regime of this study. To characterize our data, at least two velocities are needed: v_{mid}, the linear fit between 30-40 meV, and v_F, the velocity fit between 0-7 meV, as defined in Fig. 2(a). These energy ranges are chosen to get sufficient data points while avoiding the low-energy kink and 70 meV kink. v_{mid} is found to be approximately 1.8 eVÅ, without a distinct doping dependence, consistent with the previously reported 'universal' value.[1] Meanwhile, v_F *decreases monotonically with underdoping*. This is consistent with recent quantum oscillation results, which suggest a divergence of the effective mass in the underdoped regime.[21] The coupling strength of
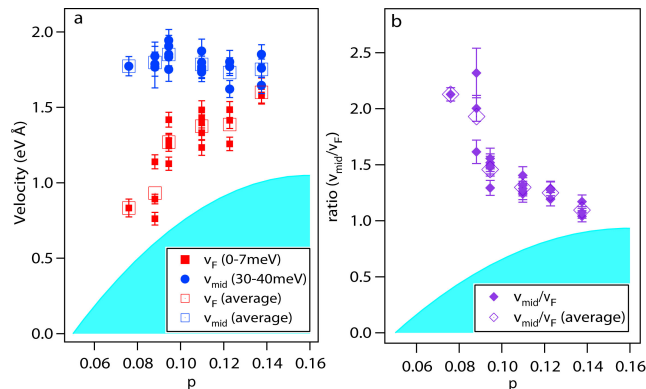
FIG. 3: (a) Doping dependence of v_F and v_{mid}. Open red (blue) squares denote average v_F (v_{mid}) for each doping. Boundary of shaded region denotes doping dependence of T_c. Doping is approximated from empirical relation T_c=96(1-82.6(p-0.16)^2).[22] v_{mid} has little systematic doping dependence, while v_F decreases with underdoping. (b) Doping dependence of v_{mid}/v_F, which is related to the renormalization coupling strength.

this low-energy renormalization can be roughly assessed by the velocity ratio v_{mid}/v_F, which is plotted in Fig. 3(b), and suggests that coupling strength increases with underdoping. Notably, the ratio of velocities on either side of the 70meV kink exhibits the same doping dependence, though with the 70 meV kink, it is the higher energy velocity (ω>70meV) which is doping-dependent.[1] Although a doping-dependent v_F presents a significant shift from our previous understanding of cuprate nodal physics, our results are not inconsistent with previous measurements: v_{mid} is indeed doping-independent, and inferior energy resolution can easily obscure subtle low-energy kinks near E_F. Our finding underscores the importance of very low energy scales in these systems and revises cuprate phenomenology by linking nodal v_F to doping and T_c, previously suggested by the temperature dependence of the low-energy kink.[7] Further, this doping dependence constrains the origin of the low-energy kink, and may aid interpretation of bulk thermodynamic measurements, particularly thermal conductivity, which will be the focus of the remaining discussion.

For the cuprates, thermal conductivity near T=0 can be expressed in terms of two components of the Fermi velocity: the velocity perpendicular to (v_F) and tangential to (v_2) the Fermi surface (FS) at the node (Fig. 4(a)-(c)).[23–25] For a 2D d-wave superconductor in the clean limit, the residual linear term (T=0 extrapolation) of thermal conductivity, κ_0/T, is independent of the quasiparticle scattering rate, interaction energy, or other sample-dependent parameters.[24, 26]

In this regime, κ_0/T is related to v_F and v_2 by a simple formula:[23, 24, 26]

$$\kappa_0/T = \frac{k_B^2}{3\hbar}\frac{n}{d}[\frac{v_F}{v_2} + \frac{v_2}{v_F}],\qquad(1)$$

where n is the number of CuO_2 planes per unit cell, and d is the c-axis unit cell length. The second term is usually negligible, as $v_2 \ll v_F$. Thus, by measuring bulk thermal conductivity, one can extract a microscopic parameter, v_2/v_F, which fully determines the ground state nodal electronic structure of cuprates.[25] Thermal conductivity measurements on $La_{2-x}Sr_xCuO_4$,[27, 28] $YBa_2Cu_3O_7$,[28] $Bi_2Sr_{2-x}La_xCuO_{6+\delta}$,[29] and Bi-2212[5] have all shown that κ_0/T decreases with underdoping, implying that v_F/v_2 also decreases. However, using v_2 reported in Ref. [30] and a universal v_F, Sun *et al* argued that ARPES suggested a different doping dependence of v_F/v_2. [5] Such contradictions have been attributed to disorder effects, such as electronic inhomogeneity [5] or disorder-induced magnetism,[6] but previous analysis lacked a crucial component: a doping-dependent v_F.

For comparisons via Eqn. (1), we have obtained v_2 from laser-ARPES measurements of the momentum dependence of the superconducting gap near the node (Fig. 4(d)), and these values are consistent with recently published data. [31, 32] Using these v_2 together with v_F from Fig. 3(a), we plot the ratio v_F/v_2 in Fig 4(f) alongside the thermal conductivity values reported by Sun *et al.*[5] The ARPES v_F/v_2 decrease strongly with underdoping, exhibiting a consistent trend with the thermal conductivity results for Bi-2212 as well as other cuprates. The v_F/v_2 derived from ARPES and thermal conductivity differ in absolute value, and this may be related to the in-plane anisotropy of thermal conductivity that has been reported in Bi-2212 ($\kappa_a \neq \kappa_b$). [5, 33] The doping-dependent data in Ref. [5] were along the *a*-axis, which has a larger κ_0/T, but the discrepancy in absolute value of v_F/v_2 shown in Fig. 4 (f) may indicate that the *b*-axis may be the correct one to compare to ARPES. Notably ARPES does not observe in-plane anisotropy of nodal single particle parameters (v_F and v_2), so the anisotropy in thermal conductivity must have a different origin, such as coexisting density-wave order.[34] Alternately, the difference in absolute value of v_F/v_2 may suggest a proportionality constant of different origin is needed in Eqn. (1). Nevertheless, with the doping-dependent v_F elucidated by laser ARPES, we are able to reproduce the doping-dependence of κ_0/T which is seen in multiple cuprate families.

The superior resolution of laser ARPES allows access to some of the lowest energy scales of high-T_c cuprates, and the findings may further constrain the microscopic theory of high-T_c superconductivity. With this powerful probe, we have been able to uncover the doping dependence of a microscopic parameter, v_F. A non-universal nodal Fermi velocity both answers old questions and introduces new ones: discrepancies between doping-dependent ARPES and thermal conductivity measurements can be resolved, but there are new questions about the origin of the low-energy kink, the explanation of its
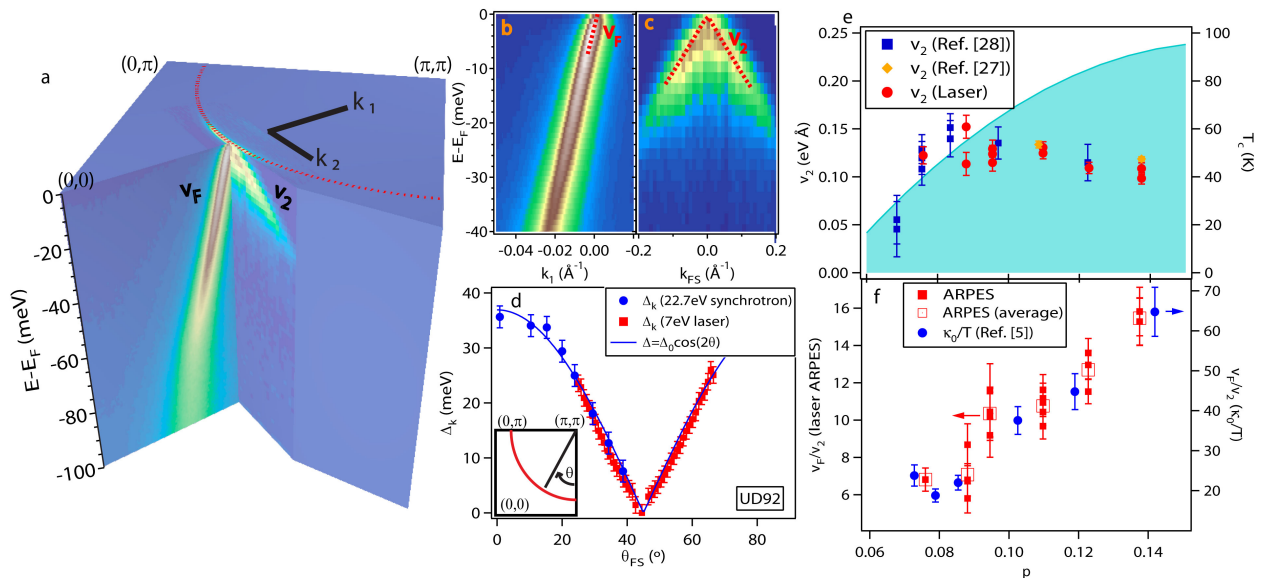
FIG. 4: (a) Cutout showing FS (top) and dispersion perpendicular (v_F, left) and tangential (v_2, right) to FS at node, from measurement on UD92 at 10K. (b)-(c) Image plots showing measured v_F and v_2 directly. The latter image consists of EDCs at k_F from many parallel cuts near the node. (d) Comparison of synchrotron- and laser-based ARPES measurements of the superconducting gap of UD92 around the FS. When the data in (d) is fit to a simple d-wave form, $\Delta(\theta)=\Delta_0\cos(2\theta)$ close to the node, $v_2 \approx 2\Delta_0/k_F$, where k_F is the distance from the node to (π,π). (e) v_2 from synchrotron- and laser-based ARPES experiments. (f) Comparison between v_F/v_2 from laser ARPES and thermal conductivity from Ref. [5]. Doping dependence is consistent, though absolute values differ. Open squares indicate average laser ARPES values.

doping and temperature dependence, and its role in superconductivity.

[1] X. J. Zhou, T. Yoshida, A. Lanzara, P. V. Bogdanov, S. A. Kellar, K. M. Shen, W. L. Yang, F. Ronning, T. Sasagawa, T. Kakeshita, et al., Nature **423**, 398 (2003).

[2] Y. Ando, S. Komiya, K. Segawa, S. Ono, and Y. Kurita, Phys. Rev. Lett. **93**, 267001 (2004).

[3] J. L. Tallon and J. W. Loram, Physica C: Superconductivity **349**, 53 (2001).

[4] T. Yoshida, X. J. Zhou, D. H. Lu, S. Komiya, Y. Ando, H. Eisaki, T. Kakeshita, S. Uchida, Z. Hussain, Z.-X. Shen, et al., J. Phys.: Condens. Matter **19**, 125209 (2007).

[5] X. F. Sun, S. Ono, Y. Abe, S. Komiya, K. Segawa, and Y. Ando, Phys. Rev. Lett. **96**, 017008 (2006).

[6] B. M. Andersen and P. Hirschfeld, Phys. Rev. Lett. **100**, 257003 (2008).

[7] N. C. Plumb, T. Reber, J. D. Koralek, Z. Sun, J. F. Douglas, K. Aiura, Y.and Oka, H. Eisaki, and D. S. Dessau, arXiv:0903.4900v3[cond-mat.supr-con] (2009).

[8] A. Lanzara, P. V. Bogdanov, X. J. Zhou, S. A. Kellar, D. L. Feng, E. D. Lu, T. Yoshida, H. Eisaki, A. Fujimori, K. Kishio, et al., Nature **412**, 510 (2001).

[9] P. Bogdanov, A. Lanzara, S. A. Kellar, X. J. Zhou, E. D. Lu, W. J. Zheng, G. Gu, J.-I. Shimoyama, K. Kishio, H. Ikeda, et al., Phys. Rev. Lett. **85**, 2581 (2000).

[10] X. J. Zhou, T. Cuk, T. Devereaux, N. Nagaosa, and Z.-X. Shen, in *In Handbook of High-Temperature Superconductivity*, edited by J. R. Schrieffer and J. S. Brooks (Springer New York, 2007), pp. 87–144.

[11] K. Ishizaka, T. Kiss, S. Izumi, M. Okawa, T. Shimojima, A. Chainani, T. Togashi, S. Watanabe, C.-T. Chen, X. Wang, et al., Phys. Rev. B **77**, 064522 (2008).

[12] W. Zhang, G. Liu, L. Zhao, H. Liu, J. Meng, X. Dong, W. Lu, J. S. Wen, Z. J. Xu, G. D. Gu, et al., Phys. Rev. Lett. **100**, 107002 (2008).

[13] J. D. Rameau, H.-B. Yang, G. D. Gu, and P. D. Johnson, Phys. Rev. B **80**, 184513 (2009).

[14] G. Liu, G. Wang, Y. Zhu, H. Zhang, G. Zhang, X. Wang, Y. Zhou, W. Zhang, H. Liu, L. Zhao, et al., Rev. Sci. Instrum **79**, 023105 (2008).

[15] P. D. Johnson, A. V. Fedorov, and T. Valla, J. Electron Spectrosc. Relat. Phenom. **117-118**, 153 (2001).

[16] M. R. Norman, M. Randeria, H. Ding, and J. C. Campuzano, Phys. Rev. B **57**, R11093 (1998).

[17] W. S. Lee, W. Meevasana, S. Johnston, D. H. Lu, I. M. Vishik, R. G. Moore, H. Eisaki, N. Kaneko, T. P. Devereaux, and Z.-X. Shen, Phys. Rev. B **77**, 140504(R) (2008).

[18] W. S. Lee, S. Johnston, T. P. Devereaux, and Z.-X. Shen, Phys. Rev. B **75**, 195116 (2007).

[19] X. J. Zhou, J. Shi, T. Yoshida, T. Cuk, W. L. Yang, V. Brouet, J. Nakamura, N. Mannella, S. Komiya, Y. Ando, et al., Phys. Rev. Lett. **95**, 117001 (2005).

[20] W. Meevasana, X. J. Zhou, S. Sahrakorpi, W. S. Lee, W. L. Yang, K. Tanaka, N. Mannella, T. Yoshida, D. H. Lu, Y. L. Chen, et al., Phys. Rev. B **75**, 174506 (2007).

[21] S. E. Sebastian, N. Harrison, M. M. Altarawneh, C. H. Mielke, R. Liang, D. A. Bonn, W. N. Hardy, and G. G. Lonzarich, arXiv:0910.2359v1 [cond-mat.str-el] (2009).

[22] J. L. Tallon, C. Bernhard, H. Shaked, R. L. Hitterman, and J. D. Jorgensen, Phys. Rev. B **51**, 12911 (1995).

[23] M. Chiao, R. W. Hill, C. Lupien, L. Taillefer, P. Lambert, R. Gagnon, and P. Fournier, Phys. Rev. B **62**, 3554 (2000).

[24] N. E. Hussey, Adv. Phys **51**, 1685 (2002).

[25] H. Shakeripour, C. Petrovic, and L. Taillefer, New Journal of Physics **11**, 055065 (2009).

[26] A. C. Durst and P. A. Lee, Phys. Rev. B **62**, 1270 (2000).

[27] J. Takeya, Y. Ando, S. Komiya, and X. F. Sun, Phys. Rev. Lett. **88**, 077001 (2002).

[28] M. Sutherland, D. G. Hawthorn, R. W. Hill, F. Ronning, S. Wakimoto, H. Zhang, C. Proust, E. Boaknin, C. Lupien, L. Taillefer, et al., Phys. Rev. B **67**, 174520 (2003).

[29] Y. Ando, S. Ono, X. F. Sun, J. Takeya, F. F. Balakirev, J. B. Betts, and G. S. Boebinger, Phys. Rev. Lett. **92**, 247004 (2004).

[30] J. Mesot, M. R. Norman, H. Ding, M. Randeria, J. C. Campuzano, A. Paramekanti, H. M. Fretwell, A. Kaminski, T. Takeuchi, T. Yokoya, et al., Phys. Rev. Lett. **83**, 840 (1999).

[31] K. Tanaka, W. S. Lee, D. H. Lu, A. Fujimori, T. Fujii, Risdiana, I. Terasaki, D. J. Scalapino, T. P. Devereaux, Z. Hussain, et al., Science **314**, 1910 (2006).

[32] W. S. Lee, I. M. Vishik, K. Tanaka, D. H. Lu, T. Sasagawa, N. Nagaosa, T. P. Devereaux, Z. Hussain, and Z.-X. Shen, Nature **450**, 81 (2007).

[33] Y. Ando, J. Takeya, Y. Abe, X. F. Sun, and A. N. Lavrov, Phys. Rev. Lett. **88**, 147004 (2002).

[34] P. R. Schiff and A. C. Durst, arXiv:0908.3168v1[cond-mat.supr-con] (2009).